Study of $\pi^- p \rightarrow \pi^- \eta(\eta) p$ at 190 GeV with the COMPASS experiment

T. Schlüter, I. Uman

on behalf of the COMPASS collaboration

Ludwig-Maximilians-Universität
Munich

XIII International Conference on Hadron Spectroscopy, Tallahassee, FL, USA
Nov.29 - Dec. 04, 2009

Agenda

- Exotic $\pi(1400)$ observations.
- Lightest scalar nonet and beyond.

Agenda

- Exotic $\pi(1400)$ observations.
- Lightest scalar nonet and beyond.
- COMPASS Detector description.
- η reconstruction.

Agenda

- Exotic $\pi(1400)$ observations.
- Lightest scalar nonet and beyond.
- COMPASS Detector description.
- η reconstruction.
- Selection and preliminary statistics of $\pi^- p \rightarrow \pi^- \eta p$
- Selection and preliminary statistics of $\pi^- p \rightarrow \pi^- \eta \eta p$

Agenda

- Exotic $\pi(1400)$ observations.
- Lightest scalar nonet and beyond.
- COMPASS Detector description.
- η reconstruction.
- Selection and preliminary statistics of $\pi^- p \to \pi^- \eta p$
- Selection and preliminary statistics of $\pi^- p \to \pi^- \eta\eta p$
- A first glimpse of $f_0(1500) \to \eta\eta$

Agenda

- Exotic $\pi(1400)$ observations.
- Lightest scalar nonet and beyond.
- COMPASS Detector description.
- η reconstruction.
- Selection and preliminary statistics of $\pi^- p \to \pi^- \eta p$
- Selection and preliminary statistics of $\pi^- p \to \pi^- \eta \eta p$
- A first glimpse of $f_0(1500) \to \eta\eta$
- PWA description and comparison with standard formalisms.

Agenda

- Exotic $\pi(1400)$ observations.
- Lightest scalar nonet and beyond.
- COMPASS Detector description.
- η reconstruction.
- Selection and preliminary statistics of $\pi^- p \to \pi^- \eta p$
- Selection and preliminary statistics of $\pi^- p \to \pi^- \eta\eta p$
- A first glimpse of $f_0(1500) \to \eta\eta$
- PWA description and comparison with standard formalisms.
- Conclusion and outlook.

Exotic $\pi(1400)$

E852

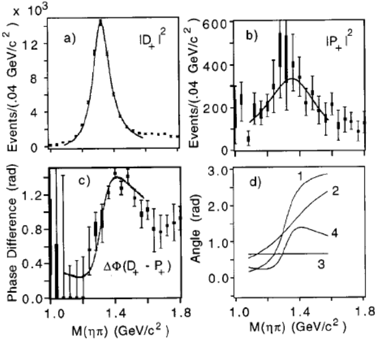

CBAR

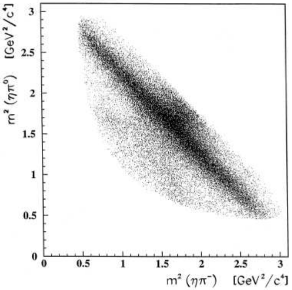

Seen by E852 exp. in $\pi^- p \to \eta\pi^- p$ at 18 GeV/c (publ. in 1997) and by CBAR exp. in $\bar{p}d \to \pi^-\pi^0\eta p_{spectator}$ (publ. in 1998).

E852

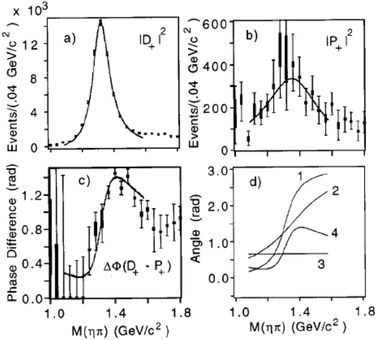

CBAR

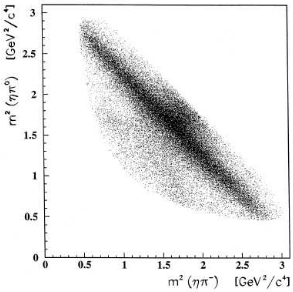

Seen by E852 exp. in $\pi^- p \rightarrow \eta\pi^- p$ at 18 GeV/c (publ. in 1997) and by CBAR exp. in $\bar{p}d \rightarrow \pi^-\pi^0\eta p_{spectator}$ (publ. in 1998).

Questioned by Dzierba et al. in 2003 in $\pi^- p \rightarrow \eta\pi^0 n$ at 18 GeV/c.

E852

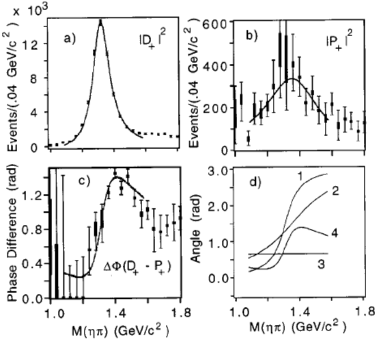

CBAR

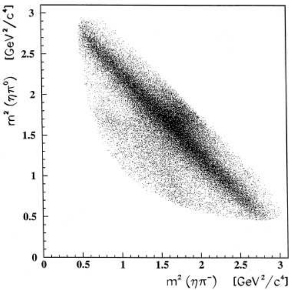

Seen by E852 exp. in $\pi^- p \rightarrow \eta\pi^- p$ at 18 GeV/c (publ. in 1997) and by CBAR exp. in $\bar{p}d \rightarrow \pi^-\pi^0\eta p_{spectator}$ (publ. in 1998).

Questioned by Dzierba et al. in 2003 in $\pi^- p \rightarrow \eta\pi^0 n$ at 18 GeV/c.

Confirmed again by E852 in 2007 in $\pi^- p \rightarrow \eta\pi^0 n$ at 18 GeV/c, but with a lower mass ($M = 1257 \pm 20 \pm 25$ MeV).

COMPASS

Hypothetical lightest scalar nonets configurations and beyond

Hypo 1 for 0^{++} Nonet

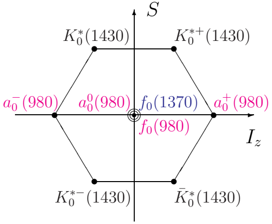

Hypo 2 for 0^{++} Nonet

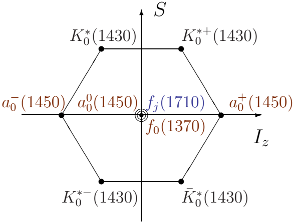

Hypothetical lightest scalar nonets configurations and beyond

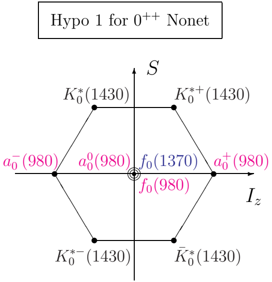

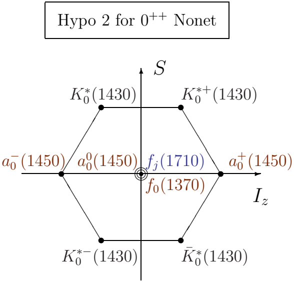

Hypo 3: $f_0(1500)$ supernumerary and therefore may be a glueball

Hypothetical lightest scalar nonets configurations and beyond

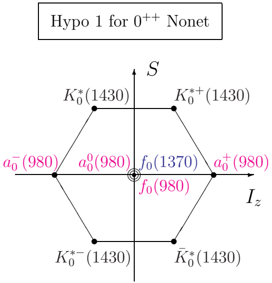

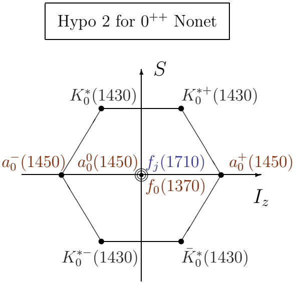

Hypo 3: $f_0(1500)$ supernumerary and therefore may be a glueball

Hypo 4: $a_0(980)$, $f_0(980)$ cusps or members of a tetraquark nonet.

Hypothetical lightest scalar nonets configurations and beyond

Hypo 1 for 0^{++} Nonet

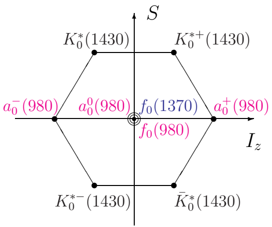

Hypo 2 for 0^{++} Nonet

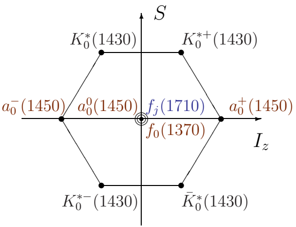

Hypo 3: $f_0(1500)$ supernumerary and therefore may be a glueball

Hypo 4: $a_0(980)$, $f_0(980)$ cusps or members of a tetraquark nonet.

Hypo 5: $f_0(1370)$, $f_0(1500)$, $f_0(1710)$ are the result of the mixing of the glueball (and a tetraquark) with ordinary mesons.

Hypothetical lightest scalar nonets configurations and beyond

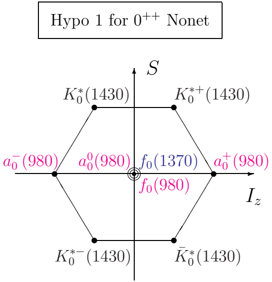

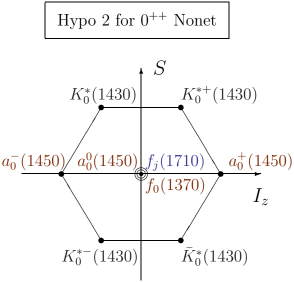

Hypo 3: $f_0(1500)$ supernumerary and therefore may be a glueball

Hypo 4: $a_0(980)$, $f_0(980)$ cusps or members of a tetraquark nonet.

Hypo 5: $f_0(1370)$, $f_0(1500)$, $f_0(1710)$ are the result of the mixing of the glueball (and a tetraquark) with ordinary mesons.

Mixing scheme is based mainly on the results of WA102 experiment.

COMPASS goal in centrally produced data is to confirm and improve the observation of WA102:

measure the decay branching widths in $K\bar{K}, \pi\pi, \eta\eta, \eta\eta', 4\pi, \eta'\eta'$, ...

Hypothetical lightest scalar nonets configurations and beyond

Hypo 1 for 0^{++} Nonet

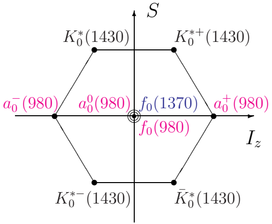

Hypo 2 for 0^{++} Nonet

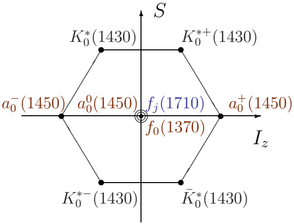

Hypo 3: $f_0(1500)$ supernumerary and therefore may be a glueball

Hypo 4: $a_0(980)$, $f_0(980)$ cusps or members of a tetraquark nonet.

Hypo 5: $f_0(1370)$, $f_0(1500)$, $f_0(1710)$ are the result of the mixing of the glueball (and a tetraquark) with ordinary mesons.

Mixing scheme is based mainly on the results of WA102 experiment.

COMPASS goal in centrally produced data is to confirm and improve the observation of WA102:

measure the decay branching widths in $K\bar{K}, \pi\pi, \eta\eta, \eta\eta', 4\pi, \eta'\eta', ...$

$\pi^- p \to \pi^- \eta\eta p$ very selective: $X \to \eta\eta$ has $I(J^{PC}) = 0(0^{++}, 2^{++}, 4^{++}, ...)$

COMPASS setup and detector description

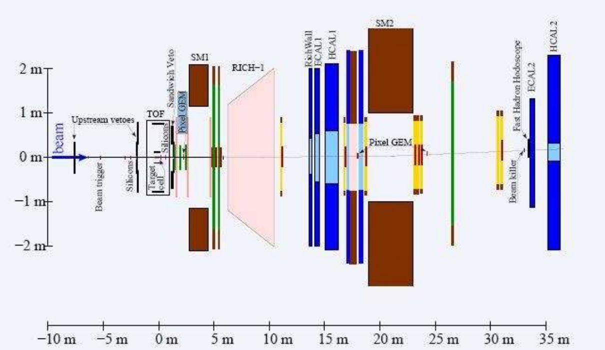

- Two arm spectrometer
- Tracking: Straw, Drift chambers, MicroMegas, PixelGEM , Recoil Proton Detector
- Calorimetry: ECAL1 (2006), ECAL2, HCAL1, HCAL2, Sandwich Veto
- Cherenkov: CEDAR, RICH

Electromagnetic Calorimeters

ECAL1

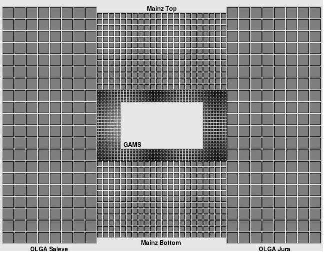

- 11.1 m downstream, low energetic photon detection, $L \times H$: $3.97 \times 2.86\ m^2$
- 1500 channels:
- OLGA: 302 cells, $14.3 \times 14.3\ cm^2$
- MAINZ: 572 cells, $7.5 \times 7.5\ cm^2$
- GAMS: 608 cells, $3.8 \times 3.8\ cm^2$

ECAL2

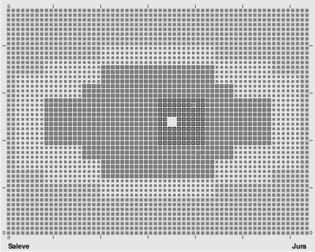

- 33.2 downstream, high energetic photon detection, $L \times H$: $2.45 \times 1.94\ m^2$
- 3068 channels:
- peripheral area: GAMS lead glass blocks $3.8 \times 3.8\ cm^2$
- central area: new $\sim$ 900 radiation hard SHASHLYK modules $3.8 \times 3.8\ cm^2$
- New ADC (2008) with 32 sample converters

Pre-selection of exclusive events

- Trigger dedicated to diffractive and "central" reactions.
- Loop to all primary vertexes.
- Interaction in the target: $-69 < z_{vertex} < -29$ cm and $r_{vertex} < 1.5$ cm.
- 1 outgoing negative track with $E_{track} < 180$ GeV.
- 2 and 4 good clusters in ECAL1 and in ECAL2 for the 2γ and 4γ channels, respectively:

Pre-selection of exclusive events

- Trigger dedicated to diffractive and "central" reactions.
- Loop to all primary vertexes.
- Interaction in the target: $-69 < z_{vertex} < -29$ cm and $r_{vertex} < 1.5$ cm.
- 1 outgoing negative track with $E_{track} < 180$ GeV.
- 2 and 4 good clusters in ECAL1 and in ECAL2 for the 2γ and 4γ channels, respectively:
    - not pointed by a track.
    - noise suppression.
    - $E_{clus_{min}} > 1$ GeV in ECAL1 and $E_{clus_{min}} > 4$ GeV in ECAL2.
    - in time with the beam: $-3 < t_{cluster} - t_{beam} < 5ns$.

Pre-selection of exclusive events

- Trigger dedicated to diffractive and "central" reactions.
- Loop to all primary vertexes.
- Interaction in the target: $-69 < z_{vertex} < -29$ cm and $r_{vertex} < 1.5$ cm.
- 1 outgoing negative track with $E_{track} < 180$ GeV.
- 2 and 4 good clusters in ECAL1 and in ECAL2 for the 2γ and 4γ channels, respectively:
  - not pointed by a track.
  - noise suppression.
  - $E_{clus_{min}} > 1$ GeV in ECAL1 and $E_{clus_{min}} > 4$ GeV in ECAL2.
  - in time with the beam: $-3 < t_{cluster} - t_{beam} < 5ns$.
- Correction of the photons momenta assuming they originate from the primary vertex.
- Correlation with RPD: $-0.3 < \phi_{\pi^- n\gamma} - \phi_p < 0.3$ rad.
- Energy balance: $180 < E_{\pi^- n\gamma} < 200\ GeV$ assuming the track to be a pion.
- $\pi^0, \eta \rightarrow \gamma_1\gamma_2$: 1 combination.
  $\pi^0_1, \eta_1 \rightarrow \gamma_i\gamma_j, \pi^0_2, \eta_2 \rightarrow \gamma_k\gamma_m$: 3 combinations.

Vertex distributions

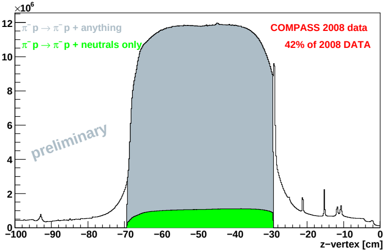

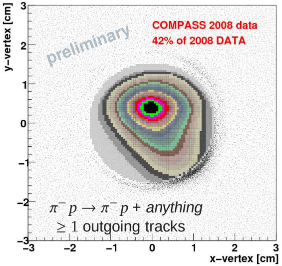

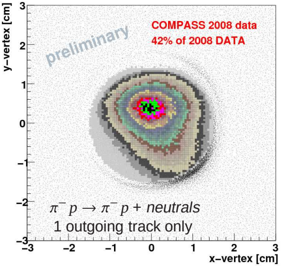

Recoil Proton Detector and exclusivity cuts

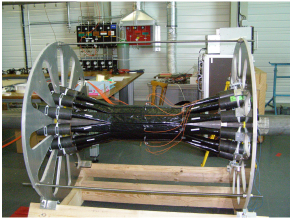

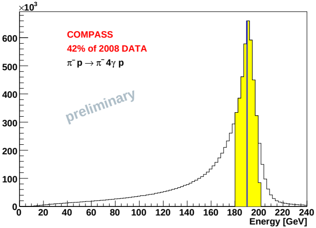

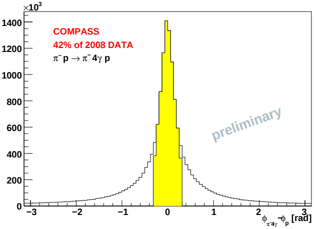

η and two-body $\eta\pi^-$ invariant masses in the 2γ channel

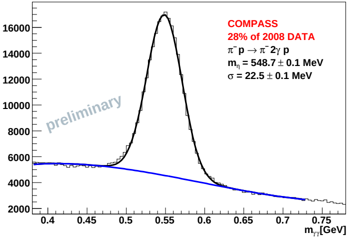

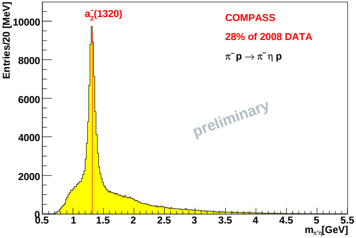

η masses in the 4γ channel

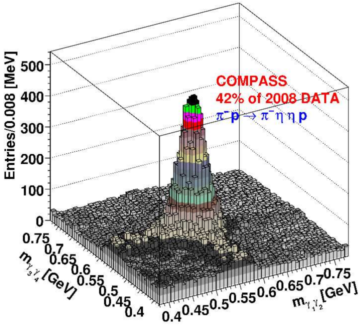

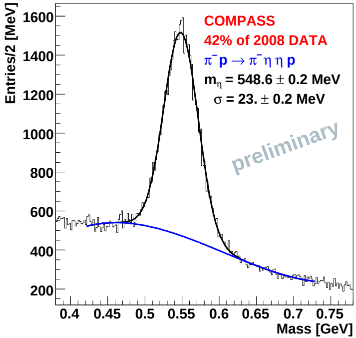

Preliminary statistics of $\pi^- p \to \pi^-\pi^0(\eta)p$

Amount of processed data (28% of 2008 data)	100.00%
DT0 trigger	73.17%
Majority < 6 for CEDAR1 and CEDAR2	71.75%
Primary vertex	66.15%
$-69 < z_{vertex} < -29$ cm	54.44%
$r_{vertex} < 1.5$ cm	52.92%
1 negative track	4.89%
Two golden clusters	0.93%
$-0.3 < \phi_{\pi^- 2\gamma} - \phi_p < 0.3$	0.25%
Exclusivity ($180 < E_{\pi^- 2\gamma} < 200\ GeV$)	0.06%
$100 < m_{\pi^0} < 170\ MeV$	31.2% of excl. events
π^0 1C $CL > 10\%$ (π^0 mass)	14.6% of excl. events
$450 < m_\eta < 650\ MeV$	21.6% of excl. events
η 1C $CL > 10\%$ (η mass)	8.1% of excl. events

- A preliminary sample of about 150K fitted $\pi^- p \to \pi^- \eta p$ events is used for the amplitude analysis.
- Better statistics will be achieved with improved calorimeter calibration (2008 data) and additional LASER and LED calorimeter monitoring system (2009 DATA).

Preliminary statistics of $\pi^- p \to \pi^- \eta\eta p$

Amount of processed data (42% of 2008 data)	100.00%
DT0 trigger	73.78%
Majority < 6 for CEDAR1 and CEDAR2	72.49%
Primary vertex	66.91%
$-69 < z_{vertex} < -29$ cm	54.81%
$r_{vertex} < 1.5$ cm	53.36%
1 negative track	4.94%
Four good clusters	0.61%
$-0.3 < \phi_{\pi^- 4\gamma} - \phi_p < 0.3$	0.21%
Exclusivity ($180 < E_{\pi^- 4\gamma} < 200\ GeV$)	0.10%
$\sqrt{(m_{\gamma_1\gamma_2} - m_{\pi^0})^2 + (m_{\gamma_3\gamma_4} - m_{\pi^0})^2} < 25$ MeV	69.78% of excl. events
$2\pi^0$ 2C $CL > 10\%$ (π^0 mass)	27.39% of excl. events
$\sqrt{(m_{\gamma_1\gamma_2} - m_{\eta})^2 + (m_{\gamma_3\gamma_4} - m_{\eta})^2} < 25$ MeV	0.17% of excl. events
2η 2C $CL > 10\%$ (η mass)	0.13% of excl. events

- A preliminary sample of about 5K fitted $\pi^- p \to \eta\eta p$ events is used for the amplitude analysis.
- Comparable amound of data is available in $\pi^- p$ and in pp at 190 GeV in the 2009 run.
- Better statistics will be achieved with improved calorimeter calibration (2008 data) and additional LASER and LED calorimeter monitoring system (2009 DATA).
- The statistics will be further increased by using the mixed decay mode of one of both ηs in $\pi^+\pi^-\pi^0$.

Two and three-body inv. masses in the 4γ channel

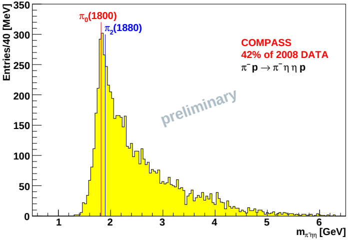

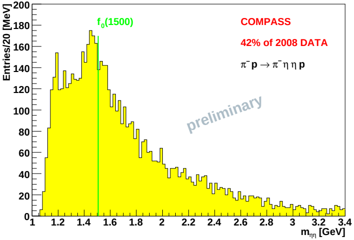

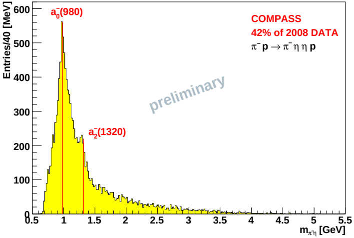

At 190 GeV incoming beam energy two compelling mechanisms for the production process of a state X are possible:

- as a product of the decay of a diffractively produced state Y: $\pi^- p \to Y p$, $Y \to \pi^- X$, $X \to \eta\eta$
- centrally produced via Double Pomeron Exchange: $\pi^- p \to \pi^-_{fast} X p$, $X \to \eta\eta$

Diffractive dissociation

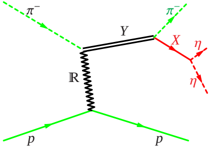

Central production

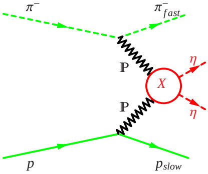

MC of diffractive dissociation

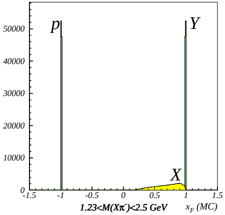

MC of central production

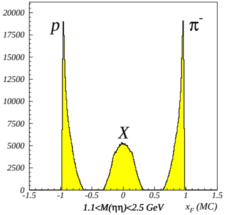

x_f and rapidities overlap: both processes have to be fitted simultaneously!

Amplitude Ansatz for the decay process

- Amplitude (isobar model):

$$A_J^\lambda = G_\lambda e^{i\delta_\lambda} F_J(q) \frac{Y_J^\lambda(\alpha,\beta)}{m_0^2 - s - i m_0 \Gamma(m)}$$

- Blatt-Weisskopf barrier factors
- Angular part: spherical harmonics,
  decay angles α,β after "Wick rotations" (no D-functions needed).
- Relativistic Breit Wigner

$$\Gamma(m) = \Gamma_0 \left(\frac{m_0}{m} \frac{q}{q_0} \frac{F_J^2(q)}{F_J^2(q_0)} \right)$$

$$w(m, m_0, m_1) = \sum_\lambda [|A^\lambda_{X_J}(m, m_0)|^2 + |A^\lambda_{Y_{J'}}(m, m_1)|^2 + 2\, c_\lambda\, \Re(A^\lambda_{X_J}(m, m_0) A^{\lambda *}_{Y_{J'}}(m, m_1)]$$

COMPASS

Amplitude Ansatz for the decay process

- Amplitude (isobar model):

$$A_J^\lambda = G_\lambda e^{i\delta_\lambda} F_J(q) \frac{Y_J^\lambda(\alpha,\beta)}{m_0^2 - s - i m_0 \Gamma(m)}$$

- Blatt-Weisskopf barrier factors
- Angular part: spherical harmonics,
  decay angles α,β after "Wick rotations" (no D-functions needed).
- Relativistic Breit Wigner

$$\Gamma(m) = \Gamma_0 \left(\frac{m_0}{m} \frac{q}{q_0} \frac{F_J^2(q)}{F_J^2(q_0)} \right)$$

$$w(m, m_0, m_1) = \sum_\lambda [|A^\lambda_{X_J}(m, m_0)|^2 + |A^\lambda_{Y_{J'}}(m, m_1)|^2 + 2\, c_\lambda\, \Re(A^\lambda_{X_J}(m, m_0) A^{\lambda *}_{Y_{J'}}(m, m_1)]$$

Amplitude Ansatz for the decay process

- Amplitude (isobar model):

$$\boxed{A_J^\lambda} = G_\lambda e^{i\delta_\lambda} \boxed{F_J(q)} \frac{\boxed{Y_J^\lambda(\alpha,\beta)}}{\boxed{m_0^2 - s - i m_0 \Gamma(m)}}$$

- Blatt-Weisskopf barrier factors
- Angular part: spherical harmonics, decay angles α,β after "Wick rotations" (no D-functions needed).
- Relativistic Breit Wigner

$$\Gamma(m) = \Gamma_0 \left(\frac{m_0}{m} \frac{q}{q_0} \frac{F_J^2(q)}{F_J^2(q_0)} \right)$$

$$w(m, m_0, m_1) = \sum_\lambda [|A^\lambda_{X_J}(m, m_0)|^2 + |A^\lambda_{Y_{J'}}(m, m_1)|^2 + 2\, c_\lambda\, \Re(A^\lambda_{X_J}(m, m_0) A^{\lambda *}_{Y_{J'}}(m, m_1))]$$

Amplitude Ansatz for the decay process

- Amplitude (isobar model):

$$A_J^\lambda = G_\lambda e^{i\delta_\lambda} F_J(q) \frac{Y_J^\lambda(\alpha,\beta)}{m_0^2 - s - i m_0 \Gamma(m)}$$

- Blatt-Weisskopf barrier factors
- Angular part: spherical harmonics, decay angles α,β after "Wick rotations" (no D-functions needed).
- Relativistic Breit Wigner
- Resonance mass dependent width

$$\Gamma(m) = \Gamma_0 \left(\frac{m_0}{m} \frac{q}{q_0} \frac{F_J^2(q)}{F_J^2(q_0)} \right)$$

- Mass of the two-body system
- Break-up momentum

$$w(m, m_0, m_1) = \sum_\lambda [|A^\lambda_{X_J}(m, m_0)|^2 + |A^\lambda_{Y_{J'}}(m, m_1)|^2 + 2\, c_\lambda\, \Re(A^\lambda_{X_J}(m, m_0) A^{\lambda *}_{Y_{J'}}(m, m_1)]$$

Amplitude Ansatz for the decay process

- Amplitude (isobar model):

$$A_J^\lambda = G_\lambda e^{i\delta_\lambda} F_J(q) \frac{Y_J^\lambda(\alpha,\beta)}{m_0^2 - s - i m_0 \Gamma(m)}$$

- Blatt-Weisskopf barrier factors
- Angular part: spherical harmonics, decay angles α,β after "Wick rotations" (no D-functions needed).
- Relativistic Breit Wigner

- Resonance mass dependent width

$$\Gamma(m) = \Gamma_0 \left(\frac{m_0}{m} \frac{q}{q_0} \frac{F_J^2(q)}{F_J^2(q_0)} \right)$$

- Mass of the two-body system
- Break-up momentum

$$w(m, m_0, m_1) = \sum_\lambda [|A^\lambda_{X_J}(m, m_0)|^2 + |A^\lambda_{Y_{J'}}(m, m_1)|^2 + 2\, c_\lambda\, \Re(A^\lambda_{X_J}(m, m_0) A^{\lambda *}_{Y_{J'}}(m, m_1)]$$

Amplitude Ansatz for the decay process

- Amplitude (isobar model):

$$A_J^\lambda = G_\lambda e^{i\delta_\lambda} F_J(q) \frac{Y_J^\lambda(\alpha,\beta)}{m_0^2 - s - i m_0 \Gamma(m)}$$

- Blatt-Weisskopf barrier factors
- Angular part: spherical harmonics, decay angles α,β after "Wick rotations" (no D-functions needed).
- Relativistic Breit Wigner

- Resonance mass dependent width

$$\Gamma(m) = \Gamma_0 \left(\frac{m_0}{m} \frac{q}{q_0} \frac{F_J^2(q)}{F_J^2(q_0)} \right)$$

- Mass of the two-body system
- Break-up momentum

$$w(m, m_0, m_1) = \sum_\lambda [|A^\lambda_{X_J}(m, m_0)|^2 + |A^\lambda_{Y_{J'}}(m, m_1)|^2 + 2\, c_\lambda\, \Re(A^\lambda_{X_J}(m, m_0) A^{\lambda *}_{Y_{J'}}(m, m_1))]$$

Amplitude Ansatz for the decay process

- Amplitude (isobar model):

$$A_J^\lambda = G_\lambda e^{i\delta_\lambda} F_J(q) \frac{Y_J^\lambda(\alpha,\beta)}{m_0^2 - s - i m_0 \Gamma(m)}$$

- Blatt-Weisskopf barrier factors
- Angular part: spherical harmonics, decay angles α,β after "Wick rotations" (no D-functions needed).
- Relativistic Breit Wigner

- Resonance mass dependent width

$$\Gamma(m) = \Gamma_0 \left(\frac{m_0}{m} \frac{q}{q_0} \frac{F_J^2(q)}{F_J^2(q_0)} \right)$$

- Mass of the two-body system
- Break-up momentum

$$w(m, m_0, m_1) = \sum_\lambda [|A^\lambda_{X_J}(m, m_0)|^2 + |A^\lambda_{Y_{J'}}(m, m_1)|^2 + 2\, c_\lambda\, \Re(A^\lambda_{X_J}(m, m_0) A^{\lambda *}_{Y_{J'}}(m, m_1))]$$

Amplitude Ansatz for the decay process

- Amplitude (isobar model):

$$A_J^\lambda = G_\lambda e^{i\delta_\lambda} F_J(q) \frac{Y_J^\lambda(\alpha,\beta)}{m_0^2 - s - im_0\Gamma(m)}$$

- Blatt-Weisskopf barrier factors
- Angular part: spherical harmonics,
  decay angles α,β after "Wick rotations" (no D-functions needed).
- Relativistic Breit Wigner

- Resonance mass dependent width

$$\Gamma(m) = \Gamma_0 \left(\frac{m_0}{m} \frac{q}{q_0} \frac{F_J^2(q)}{F_J^2(q_0)} \right)$$

- Mass of the two-body system
- Break-up momentum

- Intensity with two resonances with masses m_0 and m_1, spin J and J':

$$w(m, m_0, m_1) = \sum_\lambda [|A^\lambda_{X_J}(m, m_0)|^2 + |A^\lambda_{Y_{J'}}(m, m_1)|^2 + 2\, c_\lambda\, \Re(A^\lambda_{X_J}(m, m_0) A^{\lambda *}_{Y_{J'}}(m, m_1))]$$

- λ spin component along z, $-1 < c_\lambda < 1$ degree of coherence

Amplitude Ansatz for the decay process

- Amplitude (isobar model):

$$\boxed{A_J^\lambda} = G_\lambda e^{i\delta_\lambda} \boxed{F_J(q)} \frac{\boxed{Y_J^\lambda(\alpha,\beta)}}{\boxed{m_0^2 - s - i m_0 \Gamma(m)}}$$

- Blatt-Weisskopf barrier factors
- Angular part: spherical harmonics, decay angles α,β after "Wick rotations" (no D-functions needed).
- Relativistic Breit Wigner

- Resonance mass dependent width

$$\boxed{\Gamma(m)} = \Gamma_0 \left(\frac{m_0}{\boxed{m}} \frac{\boxed{q}}{q_0} \frac{F_J^2(q)}{F_J^2(q_0)} \right)$$

- Mass of the two-body system
- Break-up momentum

- Intensity with two resonances with masses m_0 and m_1, spin J and J':

$$\boxed{w(m, m_0, m_1)} = \sum_\lambda [|A^\lambda_{X_J}(m, m_0)|^2 + |A^\lambda_{Y_{J'}}(m, m_1)|^2 + 2\, \boxed{c_\lambda}\, \Re(A^\lambda_{X_J}(m, m_0) A^{\lambda *}_{Y_{J'}}(m, m_1)]$$

- λ spin component along z, $-1 \le c_\lambda \le 1$ degree of coherence

COMPASS

Amplitude Ansatz for the decay process

- Amplitude (isobar model):

$$A_J^\lambda = G_\lambda e^{i\delta_\lambda} F_J(q) \frac{Y_J^\lambda(\alpha,\beta)}{m_0^2 - s - i m_0 \Gamma(m)}$$

- Blatt-Weisskopf barrier factors
- Angular part: spherical harmonics, decay angles α,β after "Wick rotations" (no D-functions needed).
- Relativistic Breit Wigner

- Resonance mass dependent width

$$\Gamma(m) = \Gamma_0 \left(\frac{m_0}{m} \frac{q}{q_0} \frac{F_J^2(q)}{F_J^2(q_0)} \right)$$

- Mass of the two-body system
- Break-up momentum

- Intensity with two resonances with masses m_0 and m_1, spin J and J':

$$w(m, m_0, m_1) = \sum_\lambda [|A_{X_J}^\lambda(m, m_0)|^2 + |A_{Y_{J'}}^\lambda(m, m_1)|^2 + 2 c_\lambda \Re(A_{X_J}^\lambda(m, m_0) A_{Y_{J'}}^{\lambda *}(m, m_1)]$$

- λ spin component along z, $-1 \le c_\lambda \le 1$ degree of coherence

Amplitude Ansatz for the decay process

- Amplitude (isobar model):

$$A_J^\lambda = G_\lambda e^{i\delta_\lambda} F_J(q) \frac{Y_J^\lambda(\alpha,\beta)}{m_0^2 - s - i m_0 \Gamma(m)}$$

- Blatt-Weisskopf barrier factors
- Angular part: spherical harmonics, decay angles α,β after "Wick rotations" (no D-functions needed).
- Relativistic Breit Wigner

- Resonance mass dependent width

$$\Gamma(m) = \Gamma_0 \left(\frac{m_0}{m} \frac{q}{q_0} \frac{F_J^2(q)}{F_J^2(q_0)} \right)$$

- Mass of the two-body system
- Break-up momentum

- Intensity with two resonances with masses m_0 and m_1, spin J and J':

$$w(m, m_0, m_1) = \sum_\lambda [|A_{X_J}^\lambda(m, m_0)|^2 + |A_{Y_{J'}}^\lambda(m, m_1)|^2 + 2\, c_\lambda \Re(A_{X_J}^\lambda(m, m_0) A_{Y_{J'}}^{\lambda *}(m, m_1)]$$

- λ spin component along z, $-1 \leq c_\lambda \leq 1$ degree of coherence

Minimization and comparison with standard PWA

- Minimization of total intensity of the negative log-likelihood:

$$-ln\mathcal{L} = (-\sum_{j=1}^{N} lnw_j) + Nln(\sum_{i=1}^{M} w_i)$$

Minimization and comparison with standard PWA

- Minimization of total intensity of the negative log-likelihood:
$$-ln\mathcal{L} = (-\sum_{j=1}^{N} lnw_j) + Nln(\sum_{i=1}^{M} w_i)$$

- N: number of data events
  M: number of MC events
  Well established resonance parameters fixed at PDG values.
  $G_\lambda, \delta_\lambda, c_\lambda$: free parameters of the fit
  With this definition, and for a fixed set of parameters, a reduction of $ln\mathcal{L}$ by 0.5 is statistically significant and corresponds to one standard deviation in mass and width optimizations.
  A higher change in the $ln\mathcal{L}$ is requested for unambiguous spin determination ($\Delta ln\mathcal{L} > 10$).

Minimization and comparison with standard PWA

- Minimization of total intensity of the negative log-likelihood:

$$-ln\mathcal{L} = (-\sum_{j=1}^{N} lnw_j) + Nln(\sum_{i=1}^{M} w_i)$$

- N: number of data events
  M: number of MC events
  Well established resonance parameters fixed at PDG values.
  $G_\lambda, \delta_\lambda, c_\lambda$: free parameters of the fit
  With this definition, and for a fixed set of parameters, a reduction of $ln\mathcal{L}$ by 0.5 is statistically significant and corresponds to one standard deviation in mass and width optimizations.
  A higher change in the $ln\mathcal{L}$ is requested for unambiguous spin determination ($\Delta ln\mathcal{L} > 10$).

Main differences between this formalism and the standard PWA formalism used in the BNL E852 and WA102 experiments.

- Resonance rest frame after Wick rotation vs. Gottfried-Jackson reference frame
- Partial coherence vs. reflectivity basis with natural and unnatural-parity exchange
- Fitting procedure: unbinned log-likelihood fit vs. mass independent (binned) log-likelihood angular fit + mass fit

Minimization and comparison with standard PWA

- Minimization of total intensity of the negative log-likelihood:

  $$-ln\mathcal{L} = (-\sum_{j=1}^{N} lnw_j) + Nln(\sum_{i=1}^{M} w_i)$$

- N: number of data events
  M: number of MC events
  Well established resonance parameters fixed at PDG values.
  $G_\lambda, \delta_\lambda, c_\lambda$: free parameters of the fit
  With this definition, and for a fixed set of parameters, a reduction of $ln\mathcal{L}$ by 0.5 is statistically significant and corresponds to one standard deviation in mass and width optimizations.
  A higher change in the $ln\mathcal{L}$ is requested for unambiguous spin determination ($\Delta ln\mathcal{L} > 10$).

Main differences between this formalism and the standard PWA formalism used in the BNL E852 and WA102 experiments.

- Resonance rest frame after Wick rotation vs. Gottfried-Jackson reference frame
- Partial coherence vs. reflectivity basis with natural and unnatural-parity exchange
- Fitting procedure: unbinned log-likelihood fit vs. mass independent (binned) log-likelihood angular fit + mass fit

- Advantages:
  - high constraint fit with reduced number of non-mathematical ambiguities (useful for low statistics channel).
  - no discontinuity among different bins.

COMPASS

Minimization and comparison with standard PWA

- Minimization of total intensity of the negative log-likelihood:

$$-ln\mathcal{L} = (-\sum_{j=1}^{N} lnw_j) + Nln(\sum_{i=1}^{M} w_i)$$

- N: number of data events
  M: number of MC events
  Well established resonance parameters fixed at PDG values.
  $G_\lambda, \delta_\lambda, c_\lambda$: free parameters of the fit
  With this definition, and for a fixed set of parameters, a reduction of $ln\mathcal{L}$ by 0.5 is statistically significant and corresponds to one standard deviation in mass and width optimizations.
  A higher change in the $ln\mathcal{L}$ is requested for unambiguous spin determination ($\Delta ln\mathcal{L} > 10$).

Main differences between this formalism and the standard PWA formalism used in the BNL E852 and WA102 experiments.

- Resonance rest frame after Wick rotation vs. Gottfried-Jackson reference frame
- Partial coherence vs. reflectivity basis with natural and unnatural-parity exchange
- Fitting procedure: unbinned log-likelihood fit vs. mass independent (binned) log-likelihood angular fit + mass fit

- Advantages:
  - high constraint fit with reduced number of non-mathematical ambiguities (useful for low statistics channel).
  - no discontinuity among different bins.

- Disadvantages:
  - Computing limitations (presently fast convergence only for $< 100K$ events).
  - Additional mass and width scans for all possible spin combination of all unknown resonances needed.

Conclusion and outlook

- COMPASS first results on neutral channels with ηs.

Conclusion and outlook

- COMPASS first results on neutral channels with ηs.
- A structure at 1.5 GeV which can be associated to $f_0(1500)$ has been observed.

Conclusion and outlook

- COMPASS first results on neutral channels with ηs.
- A structure at 1.5 GeV which can be associated to $f_0(1500)$ has been observed.
- An alternative amplitude analysis has been formulated as a crosscheck to the one used for the BNL E852 and CERN WA102 experiments.

Conclusion and outlook

- COMPASS first results on neutral channels with ηs.
- A structure at 1.5 GeV which can be associated to $f_0(1500)$ has been observed.
- An alternative amplitude analysis has been formulated as a crosscheck to the one used for the BNL E852 and CERN WA102 experiments.
- MC studies has shown the equivalence of this formalism with the one used by previous experiments.

Conclusion and outlook

- COMPASS first results on neutral channels with ηs.
- A structure at 1.5 GeV which can be associated to $f_0(1500)$ has been observed.
- An alternative amplitude analysis has been formulated as a crosscheck to the one used for the BNL E852 and CERN WA102 experiments.
- MC studies has shown the equivalence of this formalism with the one used by previous experiments.
- Amplitude analysis of $\pi^- p \to \pi^- \eta(\eta) p$ real data is in progress.

Conclusion and outlook

- COMPASS first results on neutral channels with ηs.
- A structure at 1.5 GeV which can be associated to $f_0(1500)$ has been observed.
- An alternative amplitude analysis has been formulated as a crosscheck to the one used for the BNL E852 and CERN WA102 experiments.
- MC studies has shown the equivalence of this formalism with the one used by previous experiments.
- Amplitude analysis of $\pi^- p \rightarrow \pi^- \eta(\eta) p$ real data is in progress.
- The rest of 2008 and all of the 2009 data will added to the final sample.

Backup Slides

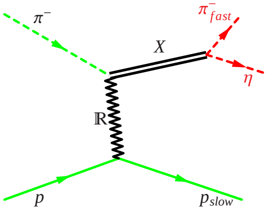

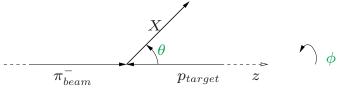

- M_X uniformly from $m_\pi + m_\eta$ to 3.5 GeV
- t_X as e^{-bt} with $b = 6\ GeV^{-2}$ with $0 < t < 1\ GeV^2$. To take into account a resonance dependent production mechanism the shape of the t-distribution will be optimized from the data in different mass ranges around the resonance masses.
- $\phi_X(\phi_p)$ uniformly from 0 to 2π

$$1 - x_X = \frac{M_X^2 - m_{\pi^-}^2}{s}$$

$$p_{T,X}^2 = -t_X$$

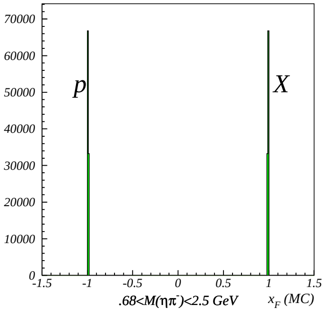

Simulation of the production of a central X in $\pi^- p \to X p$ with $X \to \eta\eta$

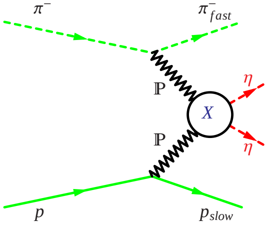

$$x_{\mathbb{P}_1} - \frac{M^2}{s}\frac{1}{x_{\mathbb{P}_1}} = \frac{M_T}{\sqrt{s}}(e^y - e^{-y})$$

Solution:

$$x_{\mathbb{P}_1} = \frac{M_T}{\sqrt{s}}\left[\pm\sqrt{\left(\frac{M_X}{M_T}\right)^2 + (\sinh y)^2} + \sinh y\right].$$

- M_X uniformly from $2m_\eta$ to 3.5 GeV
- t_X as e^{-bt} with an average $b = 6\ GeV^{-2}$ with $0 < t < 1\ GeV^2$. The optimization of a resonance dependent t-distribution will be obtained from the data.
- Flat rapidity distribution $-1 < y(X) < 1$
- $\phi_X(\phi_p)$ uniformly from 0 to 2π

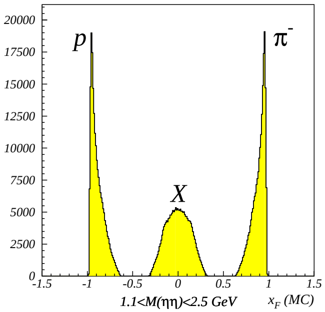

$$M_X^2 = -x_{\mathbb{P}_1} x_{\mathbb{P}_2} s$$

$x_{\mathbb{P}_2} = 1 - x_\pi$ on the π side, $x_{\mathbb{P}_1} = x_p - 1$ on the p side
In the center of mass

$$x_p + x_\pi + x_X = 0 \qquad x_X = M_T\frac{e^y - e^{-y}}{\sqrt{s}} = \frac{2M_T \sinh y_{cm}}{\sqrt{s}}$$

Wick rotation and amplitude Ansatz

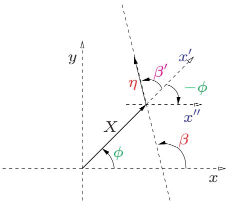

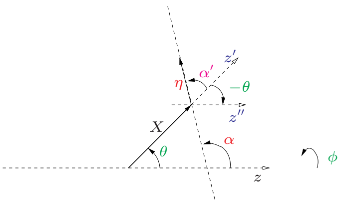

Definition of angles for a diffractive X in $\pi^- p \to \pi^- X p$, $X \to \pi^- \eta p$:

- The z axis is defined in the πp c.m. frame. The x, y axes are defined by the angle formed by the production plane and the decay plane.
- The Wick rotation by angles $-\phi$ and θ to the direction of flight of the diffractive X are followed by a Lorentz boost to the its rest frame (x', y', z') and by another rotation by $-\theta$ and $-\phi$ so that the direction of the new reference frame x'', y'', z'' correspond to one of x, y, z.
- α, β define the direction of one η in the rest frame of X after the Wick rotations. The effect of the Lorentz boost is to leave the η with final momenta different from those in the overall πp rest frame.

The angles α, β obtained in this reference frame after Wick rotations enter in the decay amplitude definition:

- $$A_J^\lambda = G_\lambda e^{i\delta_\lambda} F_J(q) \frac{Y_J^\lambda(\alpha,\beta)}{m_0^2 - s - i m_0 \Gamma(m)}$$